Experimental Thermal and Fluid Science 106 (2019) 226–233

Contents lists available at ScienceDirect

Experimental Thermal and Fluid Science

journal homepage: www.elsevier.com/locate/etfs

A new type of self-excited flapping jets due to a flexible film at the nozzle exit

M. Xu[a], M. Wu[a], J. Mi[a,b,*]

[a] Marine Engineering College, Dalian Maritime University, Dalian 116026, PR China
[b] College of Engineering, Peking University, Beijing 100871, PR China

ARTICLE INFO

Keywords:
Film flutter
Flapping jet
Oscillating jet
Self-excited nozzle
Turbulent mixing

ABSTRACT

This paper reports a new type of flapping turbulent jets that are self-excited by flutter of a flexible film with a leading edge fixed axially and centrally at a round nozzle exit. Both flutter conditions of a film and flapping-jet characteristics are investigated by varying the film material and dimensions of length (L), span (S) and thickness (δ). Visual observation, flow visualization and hot-wire anemometry are used to examine the flapping jet versus the free counterpart without involving any film. Experiments are made at $L/D = 0.5 \sim 2.0$ and the jet Reynolds number of $Re = 10{,}000$ to $50{,}000$; where $Re \equiv U_o D/\nu$ with D, U_o and ν being the jet-exit diameter, exit-averaging velocity and fluid viscosity, respectively.

Results show that the film's flutter domain reduces with increasing its overall stiffness and varies with the film's shape, size and thickness. The jet-flapping frequency f_F rises as either L decreases or U_o increases. For the rectangular FEP film of $L/D = 0.5 \sim 2.0$, the jet-flapping Strouhal number $St_F \equiv f_F D/U_o$ varies over the range of $0.05 \leq St_F \leq 0.23$. This St_F is noticeably lower than that ($\approx 0.5 \sim 0.7$) of the primary vortex passage in the non-flapping free jet, but extraordinarily one to two orders of magnitude higher than those for the self-excited oscillation of a jet from conventional fluidic nozzles.

1. Introduction

Robust control of jet mixing is desirable for many practical applications of fluid mixing. So, the management in jet mixing has long been a research topic for the community of fluid mechanics. A variety of jet control methods have been applied and studied for better mixing [1–12]. Particularly of note, during 1970–90 s, a great number of investigations of jet excitation were performed, see, e.g., Refs. [1–11]. Examples include acoustic excitation [1] and mechanical excitation involving moving parts [2–4]. These active excitation techniques have though proved quite effective in laboratory studies but are less feasible and ineffective in practical applications due to their weight, power and maintenance requirements. For practical applications, the excitation technique needs to be simple, without mechanically moving components, and yet effective. In this context, several types of practical self-exciting nozzles were developed for the enhancement of jet mixing, such as the flip-flop jet [5,6], precessing jet [7,8], and oscillating jet nozzles [9,10], as well as the "whistler" nozzles [11]. Those mechanical devices, sometimes called "fluidic" devices, naturally excite the jet itself into time-dependent self-oscillation. It has been recognised that such a dynamic self-excited oscillation significantly increases the large-scale mixing of the jet and so benefits for some practical processes. The self-exciting nozzles have found various industrial applications [12,13]. Also, the self-excited jet oscillation has attracted attention of fundamental researchers [14,15].

However, the use of fluidic nozzles is difficult to control turbulent mixing performance of the oscillating jet for different practical needs. This is because such devices are passive and cannot be modified frequently and economically for various working conditions. It is also worth noting that those self-exciting nozzles commonly cause a significant loss of energy (i.e., pressure drop) at work. This loss is mainly due to sudden expansion and/or abrupt contraction (e.g., the expansion ratio > 5, plus an outlet centre-body, for the precessing nozzle [7,8]) that the working fluid flows through. The obvious drawbacks of the fluidic device have stimulated us to seek for a new replacement that is more viable and energy-saving. Consequently, an idea occurred to us of using aerodynamic flutter of a flexible film, like a flag in wind, that may induce an entire jet oscillation. When a sufficiently strong wind blows over a sufficiently long film, an aerodynamic instability will occur and thus establish film flutter [16]. Likewise, a film fixed centrally at the nozzle exit will flutter under a sufficiently high jet speed, which is expected, in return, to excite the jet to oscillate globally. This

* Corresponding author at: College of Engineering, Peking University, Beijing 100871, PR China.
E-mail address: jmi@pku.edu.cn (J. Mi).

https://doi.org/10.1016/j.expthermflusci.2019.04.031
Received 31 October 2018; Received in revised form 12 April 2019; Accepted 30 April 2019
Available online 30 April 2019
0894-1777/

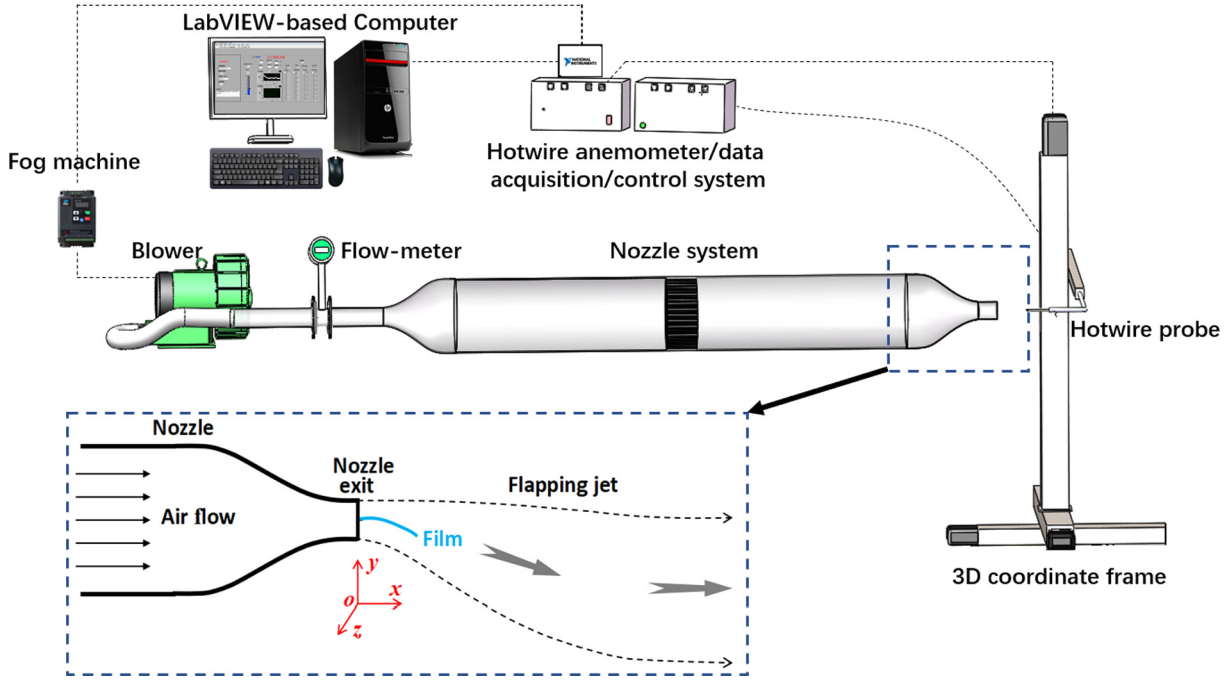

Fig. 1. Experimental facilities and schematic of a smooth contraction nozzle with a film and a flapping jet, together with the coordinate system.

speculation has indeed been corroborated by our laboratory tests [17]. In addition, we trust that the characteristics of such a jet oscillation should be quite easily modified for optimal mixing performance through artificially changing the film size, shape and location. Besides, the jet oscillation from the film-nozzle system is supposed to have less pressure loss than that from the conventional fluidic device, because a thin film placed axially at the nozzle exit may not harshly hinder the jet to discharge downstream.

Now a question arises: has any identical or similar work been conducted so far by other researchers? Our literature search has not found any previous work reporting such a new type of oscillating jets that self-excite by a film, flag or the like. Yet, as a canonical fluid–structure interaction problem, the flutter of a cantilevered flexible elastic plate has been extensively investigated [16,18–23]. See Païdoussis (2016) [18] for a complete list of references. Using a low-turbulence wind tunnel, Taneda (1968) performed a pioneering study on the flag flutter under a series of different conditions [19]. His work found that the flag flutters in various oscillation modes and also that the flutter Strouhal number depends on the oscillation mode, mass ratio, and also wind Reynolds number. It was also revealed that the critical Reynolds number for the onset of flag flutter is approximately 10^4, nearly independent of the mass ratio and Froude number. Since then, theoretical analyses and more experiments have been made on the instability of a structure (e.g., flag, paper, wooden plate, mental sheet) in a uniform flow [19–23]. Watanabe et al. [20] examined by experiment the dynamics of paper flutter in a low-speed wind tunnel. They found two primary factors, affecting the flutter speed, that are the bending stiffness and fluid-paper mass ratio. Interestingly, those authors also demonstrated the hysteresis phenomenon: i.e., the critical wind velocity for the onset of flutter during gradually speeding up the wind is greater than that at which flutter suddenly ceases as the wind velocity decreases. Later, Eloy et al. [21] conducted weakly nonlinear stability analyses and experiments with flat and curved plates to explain this phenomenon in the flag instability. These investigators revealed that the hysteresis results originally from the inherent planarity defect of the plate or film of investigation. Abderrahmane et al. [22] investigated the periodicity, quasi-periodicity and chaos of flag flutter in a flow with a relatively high turbulence-intensity.

Besides, it has become aware that the fluid–structure instability or the flutter neither derives from vortex shedding from the upstream clamp and nor it is a Kelvin–Helmholtz instability [23]. So, the film flutter, and also the jet-flapping for the present study, should be treated as a self-excited phenomenon. In principle, when the film deflects a little bit, a destabilizing pressure difference occurs across the film, while the bending stiffness tends to bring the film back to the stable planar state.

Following the above comments, the present work is designated to investigate, at the first time, a new type of flapping jets self-excited through a flexible film whose leading edge is fixed centrally at the round nozzle exit. The main objective is twofold: i.e.,

(1) To determine the jet exit conditions for film flutter to occur or the flutter domain; and
(2) To characterise the flapping jet for different film lengths against a free jet from the same nozzle without any film placed at exit.

The rest of the paper is arranged as follows. The setup and detailed conditions for experiments are provided in Section 2. The experimental results are analysed and presented in Section 3. Finally, we conclude in Section 4.

2. Experimental setup and conditions

2.1. General description

A new type of flapping jets investigated here is generated by a novel method, i.e., a jet nozzle integrating with a flexible film whose leading edge is fixed axially and centrally at the nozzle exit. Fig. 1 shows the experimental facilities, including a smoothly contracting round nozzle of the exit diameter $D = 40$ mm, to which various films can be attached, and its schematic with a film and a flapping jet. The origin of the (x,y,z) coordinates is chosen to be the center of the nozzle exit; namely, x is the downstream distance measured from the nozzle exit and y is the lateral distance from the centreline and perpendicular to the film span or width. The choice of this coordinate system results in both the flapping and non-flapping (free) jets having the identical initial conditions. Of note, the film flaps predominantly in the y direction.

By using a LabVIEW-based computer to control the frequency

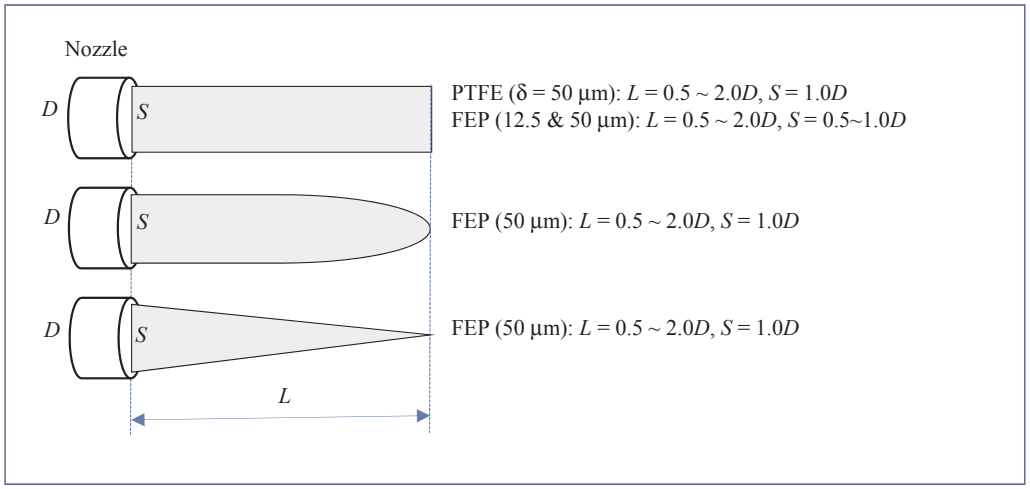

Fig. 2. Different-shaped (rectangular, semi-oval and triangular) films and their dimensions for the present study.

converter, and then to control the blower voltage through the frequency converter, the blower produces an airflow of a requested flow rate and a jet-exit speed. The blower outlet is attached to a 1.5 m long rectifier box. The rectifier box is equipped with a honeycomb grid and a metal grid. The long-section honeycomb grid parallel to the main stream can reduce fluid vorticity. The metal mesh can effectively reduce the turbulence of the airflow, suppress the possible pulsation of the incoming flow, break the large eddy (if any), and minimize the influence of the wall boundary layer on the velocity uniformity inside the chamber. The airflow through the grid can more uniformly distribute the flow and reduce the influence of the wall boundary layer, improving flow conditions and thus data quality. In the hot-wire measurements, the probe is positioned through the three-dimensional coordinate frame and control system. The x range of measurement is $x/D = 0 \sim 22$.

Fig. 2 shows the rectangular, half-elliptical and triangular films of this study and their properties. The films used are made of FEP (fluorinated ethylene propylene), with the thickness $\delta = 12.5$ & 50 μm, and PTFE (poly tetra fluoroethylene) at $\delta = 50$ μm. Six lengths of the FEP film at $\delta = 50$ μm are selected for the study, which correspond to $L/D = 0.5$, 0.75, 1.0, 1.25, 1.5 and 2.0. To properly fix the film at the nozzle exit, the 3D printing technology is utilized to make a clip with the thickness of 1.0 mm using PLA material, and fixed the film with double-sided tape. To keep the stress equally on both film sides as much as possible, the clips are placed on the two sides. Note that the excessive thickness of the clip may generate small vortices and then affect the film flutter, so the clip thickness is chosen as small as possible and clamped properly.

2.2. Flow visualisation

To identify the flapping-jet motion, a great number of instantaneous flow images of a smoked jet are taken by a Canon camera (EOS 5D Mark iii) equipped with the focal length 24–105 mm. The smoking is realized through a fog machine whose spray volume is 11.8 m^3/s with a nozzle diameter of 1.0 mm. The mixing between the working fluid and the seeding fog occurs in a reservoir located upstream of the stagnation chamber. The evergreen light source is class IV laser product for applications (532 nm wavelength, < 10 W peak power) with an exit beam diameter of about 8 mm and the exit angle of 90 degrees. The track of the laser volume is parallel to the xy plane with the illuminated region extending for about 1000 mm along the x direction and for about 500 mm along the y direction.

2.3. Hot-wire anemometry

To determine the flapping frequency f_F and compare the flapping-jet flow field with the free jet, the streamwise component of velocity (U) is measured by a single hot wire. The hot wire probe is a Wollaston wire with a diameter of 2.5 μm and the length is about 2 mm. The probe is connected to a constant temperature hot wire anemometer with an overheat ratio of 1.5. After the voltage signal is filtered and amplified, it is collected into the computer by a 12-bit A/D converter board. The sampling frequency is set at 50,000 Hz, the sampling time is 120 s. The hot-wire calibrations are performed in the jet's potential core of low turbulence intensity (≈ 0.6%) near the smooth-contraction nozzle exit before and after each set of measurements. Third polynomial curves were used to fit the calibration data, i.e., $U = a_0 + a_1E + a_2E^2 + a_3E^3$; here E is the voltage over the hot-wire when it is placed in the stream at a given velocity U measured by the pitot tube, while constants a_i ($i = 1 \sim 3$) are determined by varying 6–10 values of U. The jet exit velocity is measured by a standard pitot tube and calculated from the digital flow meter connected to the blower.

3. Results and discussion

3.1. Effective domain of flutter of a film fixed at the nozzle exit

It has been well understood that film flutter will be established from aerodynamic instability that occurs once an airflow blows over film surface at a sufficiently high velocity [16]. Likewise, when a fluid jet issues from a nozzle and flows over a film whose leading edge is fixed axially at the nozzle exit, the film is expected to flutter as the jet's speed or Reynolds number is sufficiently high, consequently inducing the jet itself to flap.

It is visually revealed on site that all the rectangular FEP films of $L/D = 0.5 \sim 2.0$ do not flutter when the jet exit velocity is below $U_o \approx 3.7$ m/s or the Reynolds number $Re < 10{,}000$. This can be explained here. In general, each film has its own stiffness that resists any displacement of it when one of its ends is fixed. To overcome the stiffness and to enable film flutter, the jet velocity has to be high enough. Indeed, as U_o increases to $U_o \geq 3.7$ m/s, film flutter occurs. Fig. 3 displays 30 photographs of a rectangular FEP film, with six different-lengths, taken at $Re = 10{,}000 \sim 45{,}000$. The exposed time is 20 s for all those xy-plane images. A close inspection can find that the flutter occurs for $L/D = 0.75 \sim 1.25$ at $Re \geq 15{,}000$ and for $L/D = 1.5 \sim 2.0$ at $Re \geq 10{,}000$. For $L/D = 0.5$, the flutter surely ensues at $Re = 45{,}000$ but the onset of flutter should happen between $Re = 32{,}000$ and $Re = 35{,}000$ or $U_o = 12 \sim 13$ m/s (see Fig. 4). In brief, as L is

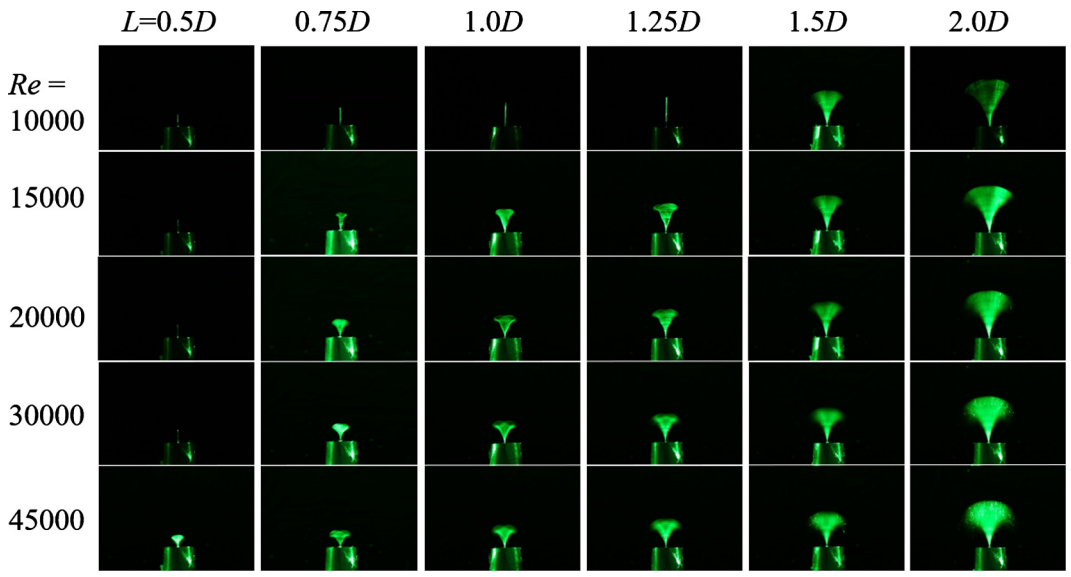

Fig. 3. Long-exposed (20 s) photographs of different-length FEP films, in the *xy*-plane, fixed at the nozzle exit.

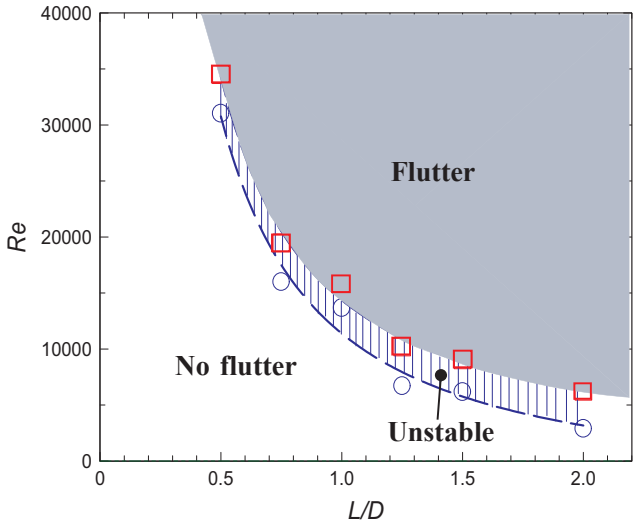

Fig. 4. Flutter domain of a FEP film at the nozzle exit: jet exit Reynolds number *Re* against *L/D*. Symbols: □, critical flutter Reynolds number Re_{cf}; ○, critical rest Reynolds number Re_{cr}.

increased, the probability for the film to flutter grows or the critical velocity (U_{cr}) for the onset of flutter drops. A likely reason for this is that the film stiffness increases with shortening *L*.

This trend is demonstrated more clearly in Fig. 4, which shows the effective domain (*Re* versus *L/D*) of flutter of a rectangular FEP film at $\delta = 50\,\mu m$. The estimates of the critical flutter Reynolds number Re_{cf} and critical rest Reynolds number Re_{cr} are based on our visual observations to each film when varying *Re*. More specifically, Re_{cf} is the value of *Re* at which film flutter starts to occur during the process of increasing *Re* through increasing U_o; on the other hand, when gradually decreasing U_o, the film returns to rest as the steady state or flutter suddenly ceases at $U_o = U_{cr}$ or $Re = Re_{cr}$. Fig. 4 demonstrates that both Re_{cf} and Re_{cr} decrease substantially with increasing *L*. For instance, when $L/D = 0.5$, Re_{cr} and Re_{cf} are approximately 31,000 and 35,000, respectively, whereas they are 3000 and 6250 for $L/D = 2.0$. Also, it is always the case where $U_{cf} > U_{cr}$ or $Re_{cf} > Re_{cr}$ regardless of *L*. This is the so-called 'hysteresis' phenomenon. Eloy et al. [21] claimed that the origin of such a hysteresis should be the inherent planarity defect of the plate or film. However, we would take this naturally as the phenomenon of inertia: it always requires a higher value of U_o to start the flutter of the motionless film than reversely to rest the fluttering film, no matter whether the film planarity is perfect or not. Certainly, the film flutter always happens for $Re \geq Re_{cf}$ but never occurs for $Re < Re_{cr}$. In the hysteresis loop, i.e., $Re_{cf} < Re < Re_{cr}$, the film is supposed to flutter intermittently. Hence, as marked on Fig. 4, the grey region is the effective domain of fully fluttering of the FEP film whereas the stripped area represents a region of unstable flutter and no flutter occurs at all in the region at $Re < Re_{cf}$.

Fig. 5 displays the relationship between the critical flutter Reynolds number Re_{cf} and the length *L* for different rectangular film properties: i.e., material FEP versus PTFE, thickness $\delta = 12.5\,\mu m$ versus 50 μm, and width $S = 0.5D$ versus $1.0D$. It is worth noting that the whole film becomes stiffer in bending either when it is made of harder material or when it is shorter, thicker or wider. In other words, the film stiffness grows with increasing the film width *S*, thickness δ and hardness but with deceasing the length *L*. It is no doubt that the flutter domain will reduce in size and Re_{cf} will rise as the stiffness grows. For instance, when using the same dimensions ($L \times S \times \delta$) of the PTFE and FEP films, the complete flutter domain for the harder one (PTFE) is smaller; concurrently its boundary shifts up and right, see Fig. 5(a). Likewise, the flutter domain shrinks when increasing the thickness and width of the FEP film, see Fig. 5(b and c).

Moreover, the flutter domain varies with the film shape, see Fig. 6. Apparently, the triangular film flutters at higher *Re* than does the rectangular one for $L < D$. This is because the former has an area twice that of the latter (see Fig. 2), which makes the former to be more easily destabilized aerodynamically. However, the situation may change for $L \geq D$, due to locally irregular aerodynamic forces acting on both sides of the films. The situation for the semi-oval film is even more complex: Re_{cf} is generally higher than that for the rectangular film at $L/D < 1.7$. Naturally, a flexible film in airflow is destabilized by different pressures exerted aerodynamically on its two sides but stabilized by its stiffness; in a highly strong flow, the aerodynamic destabilization causes a long film to flutter wildly and incoherently.

3.2. Flapping jet self-excited by film flutter

The film flutter is expected to excite the jet to flap globally. This can be confirmed qualitatively and visually by smoking the jet and quantitatively by hot-wire measurements of velocity in the downstream flow field. Fig. 7 shows those images of the smoked jets taken for the cases with a rectangular FEP film of $L = 0.75D \sim 2.0D$ and those with no film

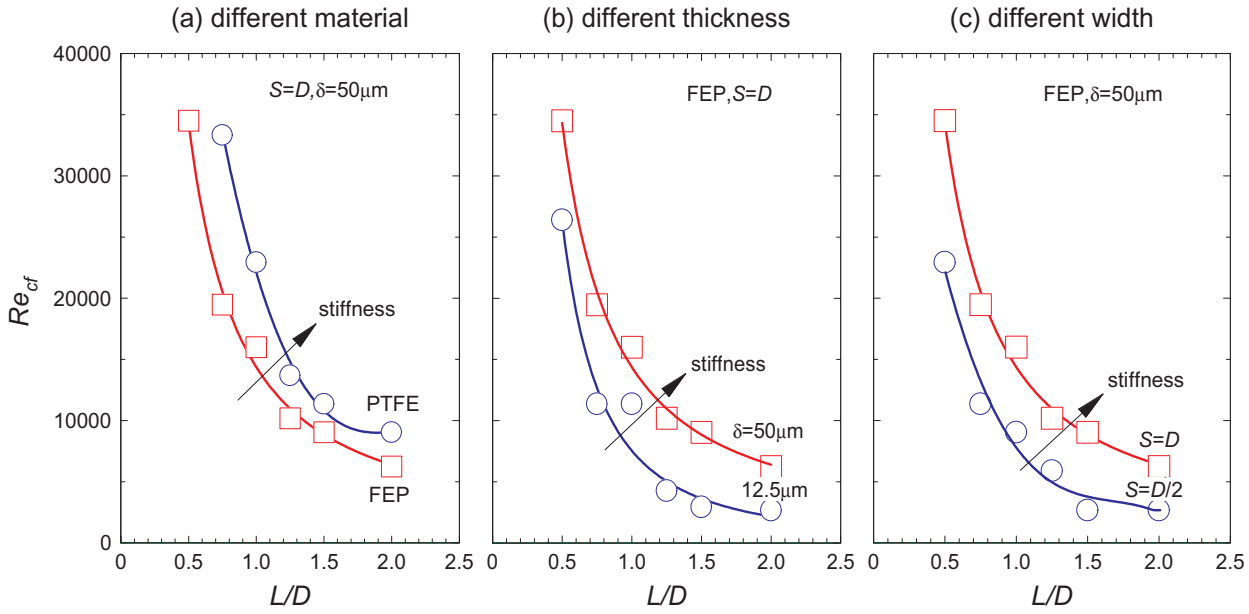

Fig. 5. Dependences of the $Re_{cf} - L/D$ relationship on the bending stiffness of a rectangular film due to different film properties: (a) material (FEP versus PTFE; δ = 50 μm, $S = 1.0D$), (b) thickness (δ = 12.5 μm versus 50 μm; FEP, $S = 1.0D$) and width ($S = 0.5D$ versus $1.0D$; FEP, δ = 50 μm).

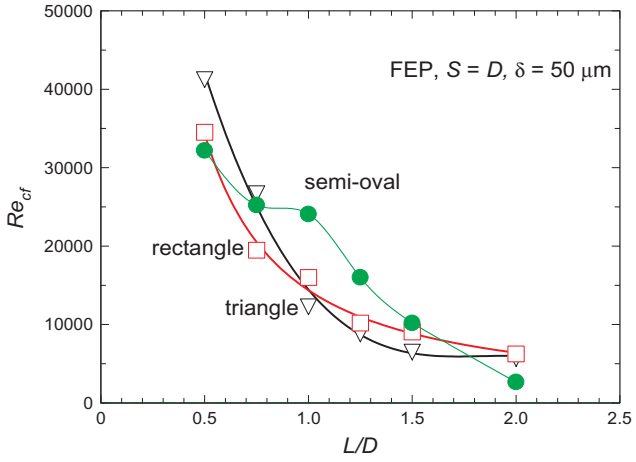

Fig. 6. Dependence of the $Re_{cf} - L/D$ relationship on the film shape.

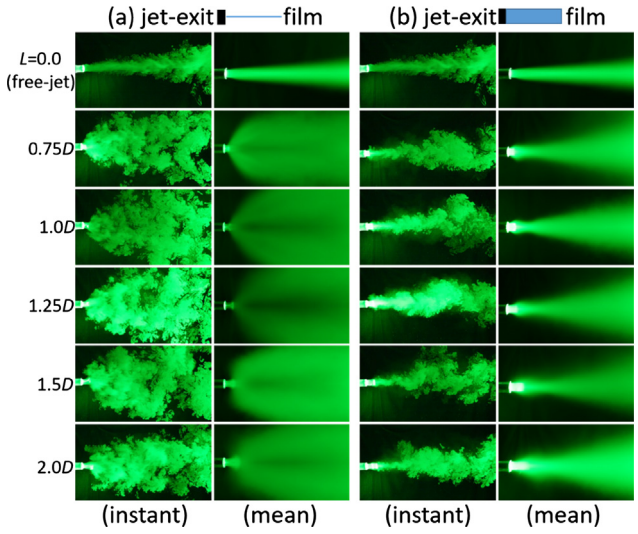

Fig. 7. Images, through (a) the *xy* plane and (b) the *xz* plane, of the smoked flapping jets excited by rectangular FEP films (δ = 50 μm) of L/D = 0.75 ~ 2.0 versus the free jet (L = 0) at Re = 30,000. The exposed time for the 'mean' images is 10 s.

or L = 0 (free jet), all at Re = 30,000. Note that the right and left images in both Fig. 7(a) and (b) are for the instantaneous and long-exposed (averaged) jet flows, respectively. Two observations can be made straightforwardly from the images:

(1) The flapping jets spread much more widely in the *xy* plane or the crosswise plane than does the non-flapping free jet, see Fig. 7(a);
(2) The flapping jets exhibit a far less spreading rate in the *xz* plane or the film spanwise plane than in the *xy* plane, despite being larger than that for the free jet.

The quantitative conformation is made in Fig. 8 that shows the velocity ratio U_e/U_c at Re = 30,000, where U_c and U_e are the local centerline mean velocity and its exit value, respectively. For reference, the present free-jet result and that of Mi & Nathan [24] obtained at Re = 15,000 are also presented on the plot. Notably, a good agreement is demonstrated between our U_e/U_c and that of Mi et al. [24], which gives a credit to the present hot-wire measurements. Indeed, as expected, the flapping jet decays, or the ratio U_e/U_c grows, much more rapidly than does the free jet. This is consistent with the spreading rate of the flapping jet being far greater than that of the free jet as seen in Fig. 7. Moreover, the careful inspection to Fig. 8 reveals that, as L is increased, the flapping-jet decay rate first rises and then drops from L/D = 1.25.

The above observations from Figs. 7 and 8 suggest undoubtedly that the flapping motion is self-excited aerodynamically through the film flutter, which leads the jet to having substantially greater large-scale mixing than does the non-flapping free jet.

3.3. Jet-flapping frequency and Strouhal number

The global jet flapping induced by the film should be somehow periodic since the previous experiments [16,18–23] have well revealed the periodicity of the film flutter. Fig. 9 indeed provides a support for this case. The figure presents the centreline power spectra (ϕ_u) of the fluctuating velocity (u) measured at x/D = 3 for the rectangular FEP film with $S = D$ and δ = 50 μm. Fig. 9(a) displays the spectrum ϕ_u

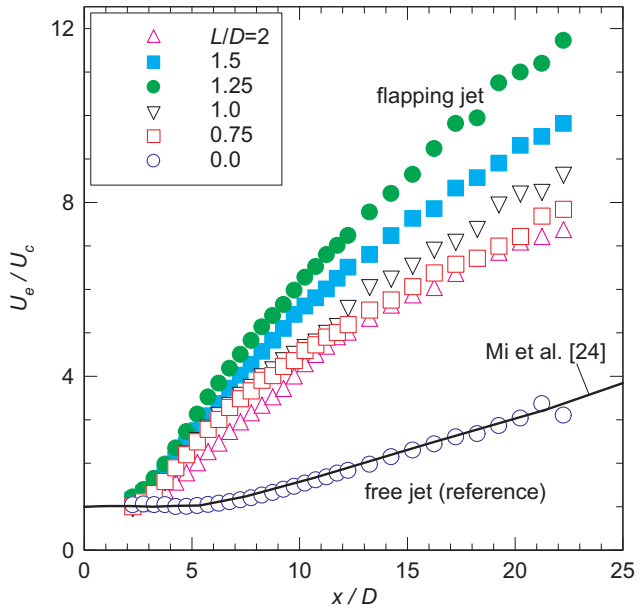

Fig. 8. The ratio of the exit-center velocity (U_e) to the centerline velocity (U_c), i.e., U_e/U_c versus x/D at Re = 30,000 for different lengths of the rectangular FEP film.

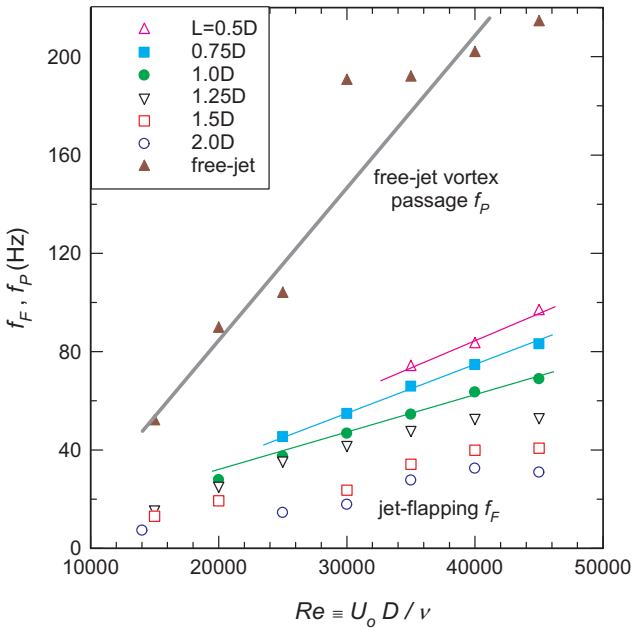

Fig. 10. Flapping frequency f_F versus Re for various lengths of a rectangular FEP film at δ = 50 μm and free-jet primary vortex passage frequency f_P versus Re.

against the frequency (f) for $Re \approx$ 30,000 when varying the film length between L/D = 0.75 and L/D = 2.0; the spectral data for the free jet are also plotted for comparison. Fig. 9(b) shows ϕ_u vs. f for L/D = 1.25 when changing the jet Reynolds number from Re = 15,000 to Re = 45,000. Evidently, the primary vortex formation induced by natural instability is revealed by a broad peak in ϕ_u for the free jet but not seen for the flapping jet. The broad peak frequency represents the passage frequency (f_P) of the primary vortex. And the peak 'broadness' implies that the vortex passage frequency varies discernibly due to numerous reasons including the merging of primary vortices formed upstream. For the flapping jet, the flapping motion is well periodic, as clearly reflected by sharp peaks or high spikes in ϕ_u. The first spike corresponds to the flapping frequency (f_F). It is also observed that f_F is significantly lower than f_P, which is expected. Besides, Fig. 9 demonstrates that f_F decreases as L grows while f_F rises with increasing Re.

Next, the dependences of the jet-flapping frequency (f_F) on the film length (L) and Reynolds number (Re) are explored. Fig. 10 shows f_F versus Re for various lengths of a rectangular FEP film at δ = 50 μm. The free-jet's f_P is also given for comparison. It is demonstrated that f_P grows with increasing Re for all L. The linear growth appears to occur for $L \leq D$. The violation of linearization for $L > D$ is expected to result from higher three-dimensionality of aerodynamics due to a long film length. The film flutter, and then the jet flapping, should become more three-dimensional as L is increased, because incoherence and inconsistence of local pressures on both sides of film are enhanced by

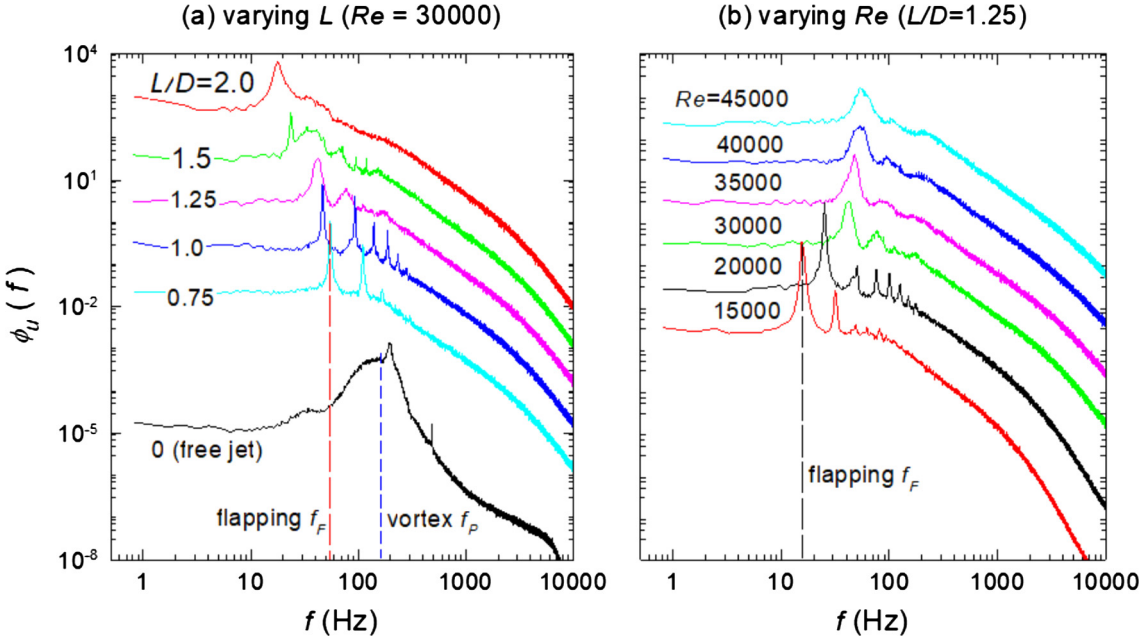

Fig. 9. Power spectra (ϕ_u) of the centreline fluctuating velocity u measured at x/D = 3 for the rectangular FEP film at $S = D$ and δ = 50 μm: (a) $Re \approx$ 30,000 and L/D = 0 ~ 2.0; (b) L/D = 1.25 and Re = 15,000 ~ 45,000. For clarity, the spectra are shifted vertically by a decade between consecutive cases of different film lengths.

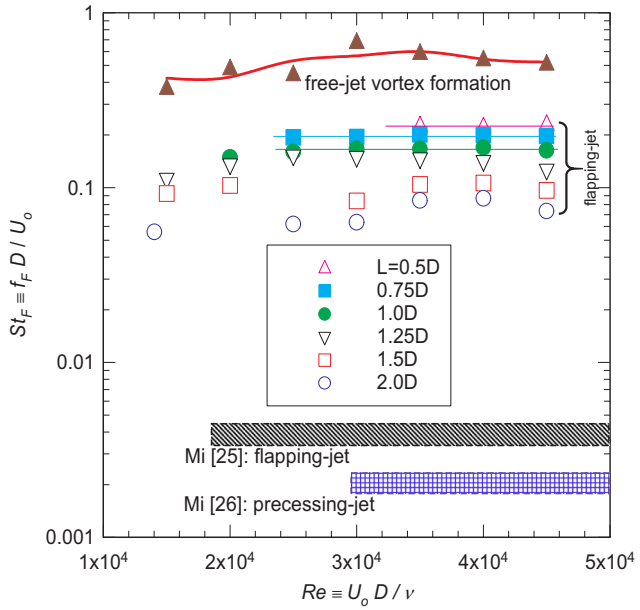

Fig. 11. Jet-flapping Strouhal number St_F versus Re for various lengths of a rectangular FEP film at $\delta = 50$ μm. The free-jet primary vortex passage Strouhal number is also given for comparison.

enlarging L. Furthermore, Fig. 10 also shows that f_F reduces as the length L grows.

Fig. 11 shows the dimensionless flapping frequency, i.e., the Strouhal number defined by $St_F \equiv f_F D/U_o$. Obviously, St_F grows as L reduces. In particular, St_F appears to be unchanged for $L/D \leq 1.0$, as marked by the horizontal lines corresponding to $St_F = 0.23$, 0.2 and 0.17 for $L/D = 0.5$, 0.75 and 1.0, respectively. For $L/D \geq 1.0$, St_F varies between 0.05 and 0.15 with $Re = 14{,}000 \sim 45{,}000$. It is worth noting that the present St_F, ranging from 0.05 to 0.23, is much greater than those of the precessing jet ($\approx 1.5 \times 10^{-3} \sim 2 \times 10^{-3}$) [25] and the flapping jet ($\approx 1.6 \times 10^{-3} \sim 3.6 \times 10^{-3}$) [26]. The jet mixing characteristics are believed to depend not only upon the jet-exit Reynolds number (Re) but also upon St_F considerably. Mi et al. [6] suggested that the dynamic flapping motion significantly enhances the large-scale mixing of the jet but concurrently may suppress the generation of the finest-scale turbulence. The extent of the suppression should be a function of St_F: i.e., the greater is St_F, the weaker is the suppression. This issue is interesting (and so will be considered as one of our studies in future) but out of the scope of this work.

4. Concluding remarks

(1) The present paper has unveiled a new type of self-excited flapping jets. Issuing from the nozzle exit with a flexible film, a turbulent jet can be 'self-excited' aerodynamically by one or more films to flap or oscillate from side to side.

(2) The critical velocity (U_{cf}) or Reynolds number (Re_{cf}) for the onset of film flutter is always greater than that (U_{cr} or Re_{cr}) for the film to rest. Namely, a hysteresis phenomenon is observed in the film flutter. Both U_{cf} and U_{cr} decrease rapidly with increasing the film length L. In the hysteresis loop, the film flutters intermittently.

(3) The domain of film flutter (the jet exit velocity U_o vs. L) reduce in size as the overall bending stiffness of film grows; that is, the domain changes with varying film shape, size and material.

(4) The jet-flapping frequency increases with either L decreasing or U_o rising. For the rectangular FEP film of $L/D = 0.5 \sim 2.0$, the flapping Strouhal number St_F varies between 0.05 and 0.23, which is considerably lower than the Strouhal number for the primary vortex formation in the free jet ($\approx 0.5 \sim 0.7$). However, St_F is one to two orders of magnitude higher than those for the self-excited oscillations of a jet from any conventional fluidic devices.

(5) Lastly, it is worthy to make a couple of additional comments on this new type of oscillating jets versus conventional fluidic nozzles. The flip-flop jet [5,6], precessing jet [7,8], and oscillating jet nozzles [9,10] were developed for modifying jet-mixing characteristics so as to meet practical needs. However, these traditional fluidic nozzles are all very passive and difficult to be manipulated for different jet's mixing performance against varying operational conditions. Also, they commonly have sudden expansion and/or abrupt contraction, thus causing substantial losses of pressure. In contrast, the present flapping jet should be easily modified artificially through altering the film size, shape and location, for optimized mixing performance. In addition, the oscillating jet from the film-nozzle system should have far less pressure loss than from the conventional fluidic device. To conclude, this new type of oscillating jets is highly likely to have significant and several advantages over the conventional fluidic nozzle for industrial applications.

Declaration of Competing Interest

We have no conflict of interest.

Acknowledgements

The authors gratefully acknowledge the joint support of the National Key Research and Development Program of China (No. 2016YFB0600605) and Natural Science Foundation of China (Grant No. 51506019).

References

[1] S.C. Crow, F.H. Champagne, Orderly structure in jet turbulence, J. Fluid Mech. 48 (1971) 547–591.
[2] J.M. Simmons, J.C.S. Lai, Jet excitation by an oscillating vane, AIAA J. 19 (1981) 673–676.
[3] M. Favre-Marinet, G. Binder, T.V. Hac, Generation of oscillating jets, J. Fluids Eng. 103 (1981) 609–613.
[4] M.R. Davis, Variable control of jet decay, AIAA J. 20 (1982) 606–609.
[5] H. Viets, Flip-flop jet nozzle, AIAA J. 13 (1975) 1375–1379.
[6] J. Mi, G.J. Nathan, R.E. Luxton, Mixing characteristics of a flapping jet from a self-exciting nozzle, Flow Turbul. Combust. 67 (2001) 1–23.
[7] G.J. Nathan, The Enhanced Mixing Burner, University of Adelaide, 1988 Ph.D Thesis.
[8] G.J. Nathan, R.E. Luxton, The entrainment and combustion characteristics and an axisymmetric, self-exciting, enhanced mixing nozzle, ASME/JSME Therm. Eng. Proc. 5 (1991) 145–151.
[9] J. Mi, G.J. Nathan, R.E. Luxton, Oscillating jets, PCT/AU98/00959, US Patent No. 6685102 (2004.2), European Pat. No. 1032789 (2004.9).
[10] G.J. Nathan, J. Mi, Z.T. Alwahabi, G.J.R. Newbold, D.S. Nobe, Impacts of a jet's exit flow pattern on mixing and combustion performance, Prog. Energy Combust. Sci. 32 (2006) 496–538.
[11] W.G. Hill, P.R. Greene, Increased turbulent jet mixing rates obtained by self-excited acoustic oscillations, ASME J. Fluids Eng. 99 (1977) 520–525.
[12] G.J. Nathan, R.E. Luxton, Flame stability and emission characteristics of the enhanced mixing burner, The 2nd European Conference on Industrial Furnaces and Boilers, April. Portugal: Algarve, (1991).
[13] C.G. Manias, G.J. Nathan, The precessing jet gas burner – a low NOx burner providing process efficiency and product quality improvements, World Cement (March) (1993) 4–11.
[14] G. Raman, D. Cornelius, Jet mixing control using excitation from miniature oscillating jets, AIAA J. 33 (1995) 365–368.
[15] M. Xu, J. Mi, P. Li, Large eddy simulations of an initially-confined triangular oscillating jet, Flow. Turbul. Combust. 88 (2012) 367–386.
[16] B.S.H. Connell, D.K.P. Yue, Flapping dynamics of a flag in a uniform stream, J. Fluid Mech. 581 (2007) 33–67.
[17] M. Wu, M. Xu, J. Mi, Experimental investigation of a flapping-jet nozzle with a flexible film at exit, in: T.C.W. Lau, R.M. Kelso (Eds.), Proceedings of the 21st Australasian Fluid Mechanics Conference (10-13 December, 2018, The University of Adelaide, Australia), Australasian Fluid Mechanics Society, 2018December 2018, ISBN 978-0-646-59784-3.
[18] M.P. Païdoussis, Fluid-Structure Interactions: Slender Structures and Axial Flow, Volume 2 Elsevier, 2016.
[19] S. Taneda, Waving motions of flags, J. Phys. Soc. Japan 24 (1968) 392–401.
[20] Y. Watanabe, K. Isogai, S. Suzuki, M. Sugihara, A theoretical study of paper flutter, J. Fluids Struct. 16 (2002) 543–560.

[21] C. Eloy, N. Kofman, L. Schouveiler, The origin of hysteresis in the flag instability, J. Fluid Mech. 691 (2012) 583–593.
[22] H. Ait Abderrahmane, M.P. Païdoussis, M. Fayed, H.D. Ng, Nonlinear dynamics of silk and Mylar flags flapping in axial flow, J. Wind Eng. Ind. Aerod. 107–108 (2012) 225–236.
[23] J. Zhang, S. Childress, A. Libchaber, M. Shelley, Flexible filaments in a flowing soap film as a model for one-dimensional flags in a two-dimensional wind, Nature 408 (2000) 835–839.
[24] J. Mi, G.J. Nathan, Statistical properties of turbulent free jets issuing from nine differently-shaped nozzles, Flow, Turbul. Combust. 84 (2010) 583–606.
[25] J. Mi, G.J. Nathan, Self-excited jet-precession Strouhal number and its influence on downstream mixing field, J. Fluids Struct. 19 (2004) 851–862.
[26] J. Mi, G.J. Nathan, Scalar mixing characteristics of a self-excited flip-flop jet nozzle, Dec. 10-14, Proc. 14th Australasian Fluid Mechanics Conference, Adelaide University, Adelaide, Australia, 2001, pp. 817–820.